

# Orbitronics for energy-efficient magnetization switching

Yuxuan YAO<sup>1†</sup>, Daoqian ZHU<sup>1,2\*†</sup>, Qingtao XIA<sup>1,3†</sup>, Jianing LIANG<sup>4</sup>, Yuhao JIANG<sup>1</sup>,  
Zhiyang PENG<sup>1</sup>, Jiayu LI<sup>1</sup>, Chen XIAO<sup>1</sup>, Renyou XU<sup>1</sup>, Wenwen WANG<sup>4</sup>,  
Xiantao SHANG<sup>4</sup>, Shiyang LU<sup>1,3</sup>, Dapeng ZHU<sup>1,3</sup>, Hong-Xi LIU<sup>4</sup>,  
Kaihua CAO<sup>1,3</sup> & Weisheng ZHAO<sup>1,2,3\*</sup>

<sup>1</sup>Fert Beijing Institute, School of Integrated Circuit Science and Engineering, Beihang University, Beijing 100191, China;

<sup>2</sup>National Key Lab of Spintronics, Institute of International Innovation, Beihang University, Hangzhou 311115, China;

<sup>3</sup>Qingdao Research Institute, Beihang University, Qingdao 266000, China;

<sup>4</sup>Truth Memory Corporation, Beijing 100088, China

Received 13 May 2024/Revised 23 June 2024/Accepted 10 October 2024/Published online 2 December 2024

**Citation** Yao Y X, Zhu D Q, Xia Q T, et al. Orbitronics for energy-efficient magnetization switching. *Sci China Inf Sci*, 2025, 68(1): 119402, <https://doi.org/10.1007/s11432-024-4186-6>

Spin-orbit torque (SOT), as a promising writing method for magnetic random-access memory (MRAM), has garnered widespread interest for over a decade [1]. Heavy metals, such as  $\beta$ -W, have been broadly adopted as spin current sources, but suffer from phase change at a limited thickness, resulting in a dramatic reduction of the charge-to-spin conversion efficiency  $\theta_{SH}$  [2]. The thickness limitation leads to stringent etching conditions and large distribution among devices, posing challenges for simultaneously satisfying SOT efficiency, etching-stop margins, and back-end-of-line (BEOL) compatibility.

The recent development of orbitronics brings new opportunities for addressing these issues by bringing novel material options [3, 4]. Orbital Hall effect (OHE) and orbital Rashba-Edelstein effect (OREE), which involve the excitation of orbital-polarized current  $J_L$  that carries orbital angular momentum  $L$  without the need for materials of a strong spin-orbit coupling (SOC), are predicted to be much stronger than their spin counterparts across diverse materials. However, the orbital angular momentum cannot directly interact with the local magnetic moment which is dominated by spin. A ‘converter’ with strong SOC, capable of transforming  $L$  into spin angular momentum  $S$ , is necessary for utilizing OHE to switch the magnetization, as shown in Figure 1(a). Different converter layers have been reported, such as Ni, garnets, and Gd, but it remains challenging to integrate these materials with magnetic tunnel junctions (MTJs). Here, we use Pt as the  $L$ -to- $S$  converter, and CoFeB or Co as the ferromagnet in our samples to show the orbital current-induced magnetic switching that is energy-efficient and MTJ compatible.

**Results.** First, we systematically investigate the effective charge-to-spin conversion efficiency  $\theta_H$  in

$X(t_X)/Pt(t_{Pt})/CoFeB(1.5)/MgO(1.5)/Ta(2)$  multilayers ( $X = Ta, Cr, W, Ru$ , units in nanometer). After deposition and annealing, we patterned the multilayers into Hall-bar devices with a width  $w = 10 \mu m$ , as shown in Figure 1(b). We then performed second harmonic Hall voltage measurements in these devices to obtain the  $\theta_H$ . The measured  $\theta_H$  for samples with  $X = Ta$  are shown in Figures 1(b) and (c). The Ta layer, which is  $\beta$ -Ta or at mixed phase, is prepared by two different conditions (see Appendix A). In samples with the  $t_{Pt}$  fixed to 2 nm, the  $\theta_H$  increases with  $t_{Ta}$ , and the highest  $\theta_H$  of  $0.152 \pm 0.003$  was obtained in Ta(12)/Pt(2), which is 1.5 times higher than that of Pt(10) and 5.6 times higher than that of Pt(2) ( $\theta_H = 0.023 \pm 0.001$ ). By fixing  $t_{Ta} = 8$  nm and varying the  $t_{Pt}$  from 0 to 10 nm, the  $\theta_H$  firstly changes its sign, increases when the Pt layer is thin, and then decreases when the Pt layer is as thick as 10 nm. The highest  $\theta_H$  reaches  $0.168 \pm 0.003$  in Ta(8)/Pt(3) bilayer. Together with the reduced  $\theta_H$  in the control sample with a MgO insertion layer, the analysis of  $\theta_H$  accounting for the current shunting effect and the XRD measurements, we attribute the underlying mechanism to the recently discovered OHE (see Appendixes B and E).

In addition to Ta/Pt, we investigated other X/Pt bilayers as SOT channels ( $X = Cr, W, Ru$ ) because all of them have been predicted to present strong orbital Hall conductivity (OHC) [5]. Consistent with the ab initio calculation results, all the X/Pt bilayers possess a positive sign of  $\theta_H$ , the same as the Pt sample (Appendix C). However, when fixing the thickness of the bilayer to X(8)/Pt(2), despite the large  $\theta_H$  discovered in the Ta/Pt bilayer, the quantified  $\theta_H$  for all the other X/Pt SOT bilayers is close to or smaller than that of Pt(10), as depicted in Figure 1(d). This unexpected result maybe due to the larger orbital diffusion length  $\lambda_{OHE}$  in Cr,

\* Corresponding author (email: daoqian\_zhu@buaa.edu.cn, weisheng.zhao@buaa.edu.cn)

† Yao Y X, Zhu D Q, and Xia Q T have the same contribution to this work.

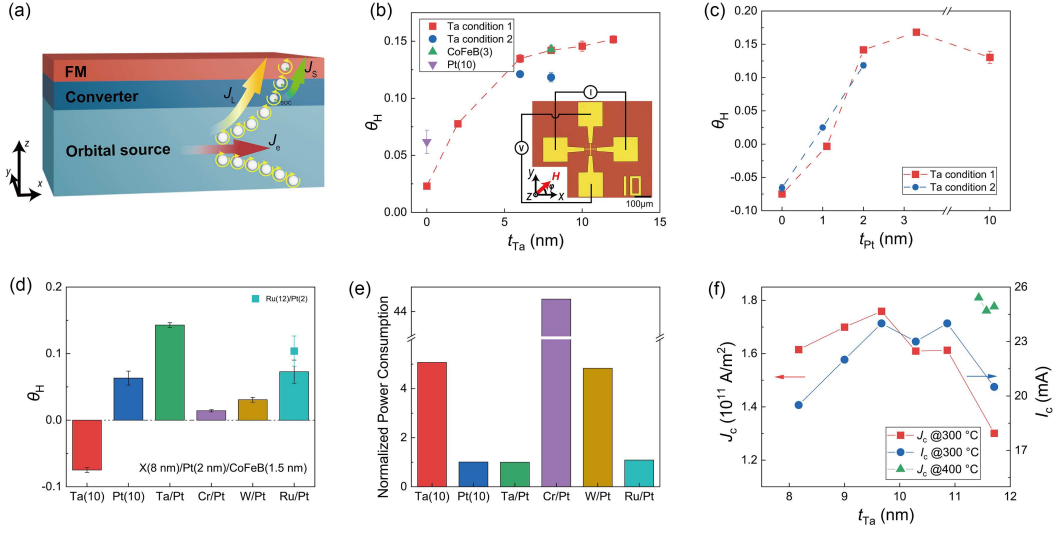


**Figure 1** (Color online) (a) Schematic of OHE-converted SOT schemes. Estimated effective charge-to-spin conversion efficiency  $\theta_H$  in different samples when varying the thickness of (b) Ta and (c) Pt. Inset in (b) is the optical image of a Hall-bar device. (d) Estimated  $\theta_H$  and (e) calculated power consumption of Ta(10), Pt(10), and X(8)/Pt(2) SOT channels. (f) Critical current density  $J_c$  and critical current  $I_c$  for Ta/Co/Pt devices with varying  $t_{Ta}$  after annealing at 300°C or 400°C.

Ru and W since the calculated OHCs in these materials are all larger than that of  $\beta$ -Ta. Adopting  $\rho_{xx}/\theta_H^2$  as a criterion, we evaluated the power consumption for these SOT channels. Normalized by the value of Ta(8)/Pt(2), as shown in Figure 1(e), the Ta/Pt and Ru/Pt bilayers emerge as the optimized choice for SOT channels.

Based on our findings, we further investigated the SOT-induced perpendicular magnetization switching in Ta(8-12)/Pt(2)/Co(0.65) due to its optimized  $\theta_H$  (Appendix D). The perpendicular anisotropy field  $\mu_0 H_K$  was validated to be  $\sim 0.25$  T ( $\sim 1$  T) after annealing at 300°C (400°C), we summarize the critical switching current  $I_c$  and current density  $J_c$ , as shown in Figure 1(f). The  $J_c$  generally decreases with the thickness of Ta thanks to the increasing  $\theta_H$  in the Ta/Pt bilayer, and the  $J_c$  for the device with  $t_{Ta} = 11.7$  nm is only  $\sim 1.3 \times 10^{11} \text{ A} \cdot \text{m}^{-2}$ , much lower than that of the reported Pt/Co bilayers. The  $I_c$  for Ta(8)/Pt(2) and Ta(12)/Pt(2) remains nearly the same, thus helping solve the etching-stop issue. Further, the SOT-induced switching remains robust after annealing at 400°C and the  $J_c$  is just slightly increased despite the  $\mu_0 H_K$  being substantially enhanced, which is of practical interest for the development of BEOL compatible SOT-MRAM.

**Conclusion.** In summary, we have systematically investigated the effective charge-to-spin conversion efficiency  $\theta_H$  in X/Pt/CoFeB/capping layer (X = Ta, Cr, W, Ru). We achieve an enhanced  $\theta_H$  brought by orbital currents, which reaches  $0.168 \pm 0.003$  in the Ta/Pt/CoFeB/capping layer and 0.1 in the Ru/Pt/CoFeB/capping layer. We have validated that the Ta/Pt bilayer is an optimized material choice for energy-efficient SOT switching, which even withstands the 400°C annealing process. Our work paves the way for the practical implementation of orbitronics, and creates

novel prospects for energy-efficient SOT-MRAM with enhanced etch-stop margins and low distribution among devices.

**Acknowledgements** This work was supported by National Key Research and Development Program of China (Grant Nos. 2022YFB4400200, 2022YFA1402604), National Natural Science Foundation of China (Grant Nos. 92164206, 52121001, 62404013, T2394472, T2394474), Beijing Natural Science Foundation (Grant No. L234081), New Cornerstone Science Foundation through the XPLOER PRIZE, National Postdoctoral Program for Innovative Talents (Grant No. BX20220374), and Fundamental Research Funds for the Central Universities (Grant No. KG16254501). The authors thank the technical support from Truth Instruments Co., Ltd. and Truth Equipment Co., Ltd. for their high-precision spintronic device prober and sputtering system.

**Supporting information** Appendixes A–E. The supporting information is available online at [info.scichina.com](http://info.scichina.com) and [link.springer.com](http://link.springer.com). The supporting materials are published as submitted, without typesetting or editing. The responsibility for scientific accuracy and content remains entirely with the authors.

## References

- 1 Yao Y, Cheng H, Zhang B, et al. Tunneling magnetoresistance materials and devices for neuromorphic computing. *Mater Futures*, 2023, 2: 032302
- 2 Honjo H, Nguyen T V A, Watanabe T, et al. First demonstration of field-free SOT-MRAM with 0.35 ns write speed and 70 thermal stability under 400°C thermal tolerance by canted SOT structure and its advanced patterning/SOT channel technology. In: Proceedings of the IEEE International Electron Devices Meeting (IEDM), 2019
- 3 Choi Y G, Jo D, Ko K H, et al. Observation of the orbital Hall effect in a light metal Ti. *Nature*, 2023, 619: 52–56
- 4 Zheng Z, Zeng T, Zhao T, et al. Effective electrical manipulation of a topological antiferromagnet by orbital torques. *Nat Commun*, 2024, 15: 745
- 5 Salemi L, Oppeneer P M. First-principles theory of intrinsic spin and orbital Hall and Nernst effects in metallic monoatomic crystals. *Phys Rev Mater*, 2022, 6: 095001